Molecular Catalysis 550 (2023) 113607

Contents lists available at ScienceDirect

Molecular Catalysis

journal homepage: www.journals.elsevier.com/molecular-catalysis

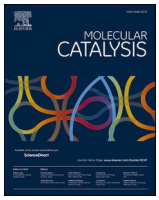

Nitrate radicals generated by TiO_2 heterogeneous photocatalysis: Application to the cleavage of C=C double bond to carbonyl compounds

Alessandro Gottuso [a], Claudio De Pasquale [b], Stefano Livraghi [c], Leonardo Palmisano [d], Sandra Diré [a], Riccardo Ceccato [a], Francesco Parrino [a,*]

[a] Department of Industrial Engineering, University of Trento, Via Sommarive 9, 38123 Trento, Italy
[b] Department of Agricultural, Food and Forest Sciences, University of Palermo, Viale delle Scienze Ed. 4, 90128 Palermo, Italy
[c] Department of Chemistry and NIS Centre, University of Torino, Via Pietro Giuria 7, 10125 Torino, Italy
[d] Department of Engineering, University of Palermo, Viale delle Scienze Ed. 6, 90128 Palermo, Italy

ARTICLE INFO

Keywords:
Nitrate radicals
TiO_2 photocatalysis
C=C oxidative cleavage
Silver nitrate
Limonene

ABSTRACT

The oxidative cleavage of alkenes represents a relevant chemical process with immense potential for the synthesis of partially oxidized compounds. Several methodologies have been proposed for achieving oxidative cleavage of alkenes, aiming to obtain carbonyl products. However, none of these approaches have been successfully scaled up for industrial applications beyond the laboratory scale. In this study, we report the selective photocatalytic oxidative cleavage of limonene to limononaldehyde using irradiated TiO_2 suspensions in the presence of silver nitrate under ambient conditions. Results demonstrate that within one hour of irradiation, a notable conversion and selectivity of 60% towards limononaldehyde can be achieved. The investigation reveals that the oxidation process is primarily driven by nitrate radicals, generated through hole-induced oxidation of nitrate ions. Notably, this selective photocatalytic approach shows potentials that bode well for its application to other olefinic substrates in addition to limonene. These results present a promising pathway for the scalable industrial synthesis of partially oxidized compounds through selective photocatalytic oxidation of alkenes.

1. Introduction

Alkenes are considered to be among the most relevant compounds for modern industrial chemistry, because of their suitability as starting compounds for a broad variety of reactions, including electrophilic substitution/addition, hydrogenation and oxidation [1]. In the presence of a strong oxidizing agent, the double bond of alkenes can be oxidatively cleaved, producing industrially relevant carbonyl compounds [2, 3]. On top of that, particularly interesting is the oxidative cleavage of cyclic olefins, as it is possible to obtain bi-functionalized α,ω-compounds, which can be used as precursors for plasticizers, resins and polymers, such as polyamides and polyurethanes [4]. Several methods have been proposed for the oxidative cleavage of alkenes; many of these involve the use of stoichiometric amounts of environmentally unfriendly oxidizing agents such as $KHSO_5$ (oxone) [5], $KMnO_4$ [6], $NaIO_4$ [7], Cr salts [8], m-chloroperbenzoic acid [9], and hypervalent iodine [10]. Other processes take place in the presence of noble-metal-based catalysts (Ir, Pd, Au, Os) [11], porphyrin derivatives [12], or enzymes [3]. An alternative is ozonolysis, a process in which ozone adds as an electrophile to an alkene to give the unstable cyclic molozonide, which immediately rearranges to the more stable ozonide. The latter is easily transformed to the corresponding carbonyl products when in the presence of a reducing agent such as zinc or dimethyl sulfide [13]. Another method involves the use of singlet oxygen for [2 + 2] cycloaddition reactions, which, unfortunately, applies effectively only to electron-rich carbon-carbon double bonds [14]. Most of the mentioned methods are mainly used at lab scale, and present relevant issues when implemented at larger scale. On the other hand, the main process industrially implemented, i.e. hydroformylation, requires harsh conditions (temperatures and pressures up to 200 °C and 100 atm, respectively), homogeneous Rh or Co catalysts, and stoichiometric amounts of syngas, which mainly derives from steam reforming or partial oxidation of natural gas or liquid hydrocarbons [15]. Therefore, alternative methods based on heterogeneous catalytic systems, operating under mild conditions are urgently required in view of a more green and sustainable industrial production. These features are displayed by the photocatalytic approach, which has recently proved to be a mature technology for the green and sustainable synthesis of

* Corresponding author.
E-mail address: francesco.parrino@unitn.it (F. Parrino).

https://doi.org/10.1016/j.mcat.2023.113607
Received 8 March 2023; Received in revised form 29 June 2023; Accepted 18 September 2023

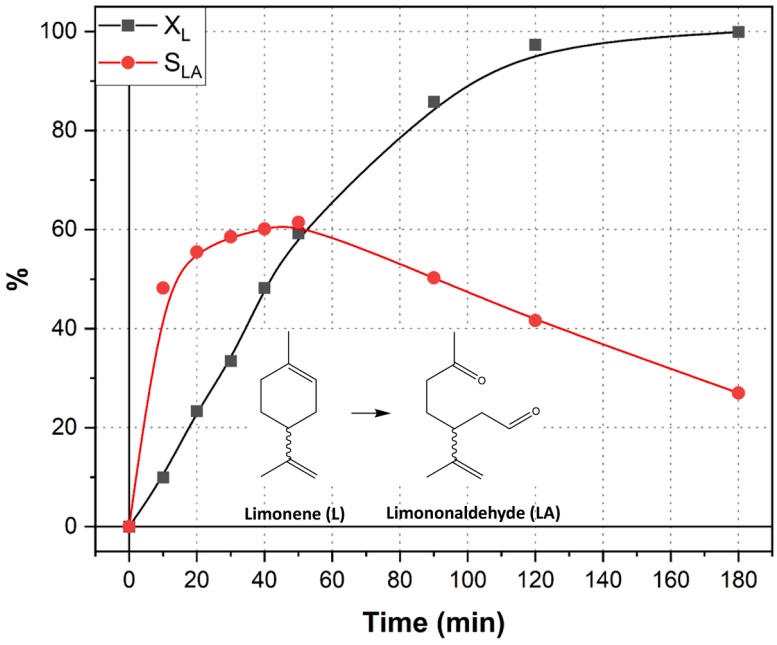

Fig. 1. Limonene conversion (X_L, black squares), selectivity to limononaldehyde (S_{LA}, red circles), versus irradiation time for a representative run.

high-added value compounds [16]. Heterogeneous photocatalysis relies on the property of irradiated semiconductors (such as TiO_2) to promote photogeneration of electrons (e^-) and holes (h^+) (Eq. (1)), which eventually transfer to electron acceptors (A) or donors (D), respectively (Eq. (2)), giving rise to useful chemical transformations [17].

$$TiO_2 + hv \rightarrow TiO_2*(e^-CB, h^+CB) \quad (1)$$

$$TiO_2*(e^-CB, h^+CB) + A + D \rightarrow TiO_2 + A^{-\bullet} + D^{+\bullet} \quad (2)$$

Few examples of photocatalytic C=C cleavage have been recently reported in the presence of $ZnIn_2S_4$ and thiol as initiator [18], by exploiting a mechanistically similar process carried out in homogeneous phase in the presence of disulfides [19]. Similar results have been obtained in the presence of carbon nitride using N-hydroxysuccinimide [20] as mediator, and of $Bi_4O_5Br_2$ [21]. Most of these papers report on oxidative cleavage of aryl substituted double bonds. To the best of our knowledge, the heterogeneous photocatalytic cleavage of olefinic double bond to carbonyl compounds in the presence of TiO_2 have been never reported up to now. Results suggest that this reaction, which is also the object of a pending patent [22], applies to both aryl- and alkyl-substituted C=C double bonds, and is selectively triggered by nitrate radicals ($NO_3^{\bullet}$) produced through photocatalytic oxidation of nitrate ions. It is worth noting that the existence of nitrate radicals in photocatalytic systems has been only recently proposed [23], thus this reaction constitutes a further demonstration of their existence in heterogeneous photocatalysis, and one of their first applications in the field of photocatalytic organic synthesis [24,25].

2. Experimental

Titanium dioxide (P25 Evonik, anatase (73–85%), rutile (14–17%), amorphous (0–13%)) [26], lithium nitrate ($LiNO_3$, 99.0%, Sigma-Aldrich), silver nitrate ($AgNO_3$, 99.8%, Carlo Erba), (*R*)-limonene ($d = 0.844$ g/mL, 97%, Sigma-Aldrich), cyclohexene ($d = 0.811$ g/mL, > 99.0% Sigma-Aldrich), styrene ($d = 0.909$ g/mL, 99.9% Sigma-Aldrich), *trans*-stilbene (96%, Sigma-Aldrich), *trans*-4-octene ($d = 0.715$ g/mL, 98%, Sigma-Aldrich), 2-cyclohexen-1-one ($d = 0.993$ g/mL, >95%, Sigma-Aldrich), 1-octene ($d = 0{,}715$ g/mL, 98%, Sigma-Aldrich), acetonitrile ($d = 0.780$ g/mL, anhydrous, 99.8%, Sigma-Aldrich), ethanol ($d = 0.789$ g/mL 99.8%, Fluka) were used as received without further purification.

In a representative run, 15 mg of TiO_2 (Evonik P25, 0.5 g/L) were dispersed in 30 mL of a solution containing $AgNO_3$ (Sigma-Aldrich, 10 mM) and limonene (R-limonene, Sigma-Aldrich, 2 mM) in acetonitrile. Then, the mixture was sonicated for 15 min, vigorously stirred and irradiated by UV-A light under static air in a Pyrex reactor equipped with six actinic lamps (15 W each). Samples were withdrawn at fixed times, filtered, and quantitatively analysed by means of GC/MS. Details on compounds identification and quantification are reported in Supplementary Information, SI, S1–3.

High-resolution Transmission Electron Microscopy (HRTEM) images were obtained on a JEOL 3010-UHR instrument (acceleration potential: 300 kV) equipped with an EDAX probe. Samples for TEM investigation were supported onto a holed carbon coated copper grid by dry deposition.

The UV–vis diffuse reflectance spectrum of the photocatalyst after a representative run was recorded by using a Varian Cary 5000 spectrometer. A Polytetrafluoroethylene (PTFE) sample was used as the reference. The spectrum was recorded in the 200–800 nm range at a scan rate of 240 nm/min with a step size of 1 nm. The measured reflectance was converted with the Kubelka-Munk function.

Powder X-ray Diffraction (PXRD) patterns were obtained using a diffractometer in Bragg–Brentano geometry equipped with a Cu anode source (Kα, $\lambda = 1.54056$ Å, voltage 40 kV, current 30 mA) coupled to a multilayer collimating monochromator (Goebel mirror). Samples were positioned in reflection geometry with a fixed angle of 10° with respect to the incident beam and the diffraction patterns were acquired by means of a Dectris Mythen 1 K hybrid pixel detector with typical 10–100° 2θ range, steps of 0.05° and acquisition time of 5 s/step. The instrument resolution (divergent and antiscatter slits of 0.5°) was determined using standards free from the effect of reduced crystallite size and lattice defects. Phase identification and Rietveld refinement of

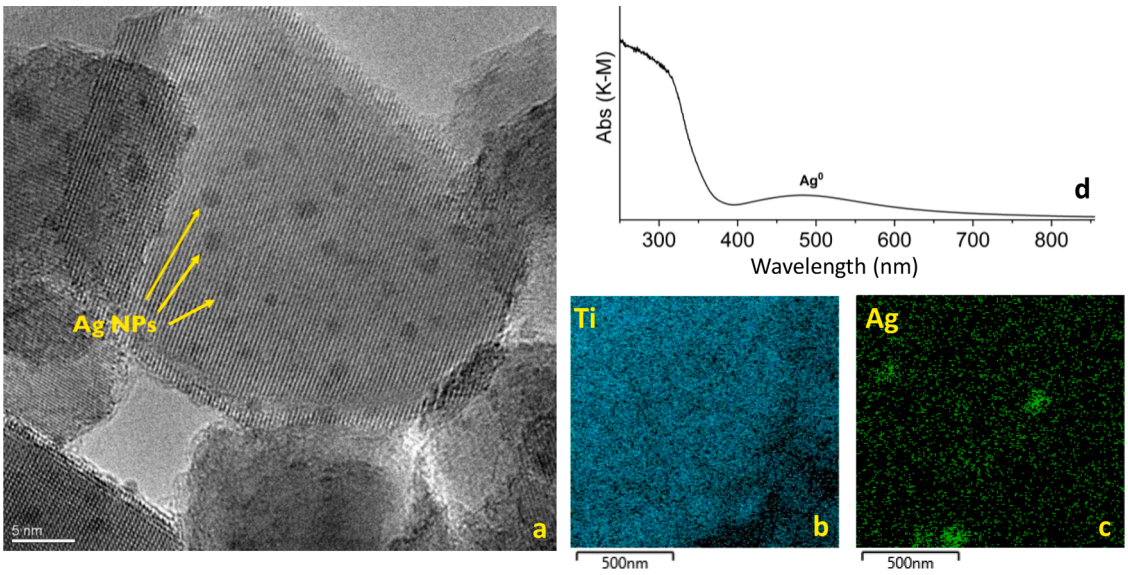

Fig. 2. a: HR-TEM image of the TiO_2 photocatalyst recovered after 180 min of UV-A irradiation in the presence of $AgNO_3$ 10 mM and (*R*)-limonene 2 mM in acetonitrile. Silver nanoparticles (Ag NPs) are highlighted with yellow arrows; b: EDX map of titanium atoms (light blue points); c: EDX map of silver atoms (green points); d: UV–vis diffuse reflectance spectrum (DRS) of the same sample.

the diffraction patterns were performed by means of QualX 2.0 and MAUD 2.33 (Material Analysis Using Diffraction) suites of program, respectively [27].

Repeatability tests were performed as it follows. The photocatalyst used for a representative run was separated through centrifuge, washed with a water-ethanol solution (50% v/v) several times, dried overnight at 70 °C and reused for the following run after adding 10 mM $LiNO_3$ as the nitrate source, without further addition of silver ions.

Details on the Griess method used to detect NO_2 are described in Section S4.

3. Results and discussion

The values of limonene conversion (X_L) and selectivity towards limononaldehyde (S_{LA}) versus irradiation time in the presence of bare TiO_2 and $AgNO_3$ are reported in Fig. 1, along with the related reaction scheme.

Limonene is fast oxidized, reaching almost total conversion during three hours of irradiation. Production of limononaldehyde (LA) occurs with a maximum selectivity of ca. 60% after 50 min. Thereafter, selectivity decreases, in agreement with what reported in literature for other partial oxidation processes in batch systems [28]. Notably, only the endocyclic double bond undergoes cleavage, while the exocyclic one is stable under the present reaction conditions. It is crucial to highlight that the primary oxidation product of limonene is limononaldehyde, as evidenced by the chromatogram presented in Supporting Information (Fig. S2). However, several much smaller peaks, difficult to quantify, are also discernible, which likely originate from direct hole-induced oxidation of limonene (as in the case of limonene conversion in the absence of nitrate) or from overoxidation of limononaldehyde. Blank tests carried out under dark conditions or in the absence of TiO_2 did not result in limonene degradation, thus indicating the photocatalytic nature of the reaction. Moreover, the reaction did not appreciably take place under nitrogen atmosphere.

In order to assess the role of silver and nitrate ions, control runs were carried out under otherwise similar conditions but (i) in the absence of $AgNO_3$, (ii) with equimolar amounts of $AgClO_4$ or (iii) $LiNO_3$. For all of these tests, limonene concentration rapidly decreased, but only negligible production of limononaldehyde was detected, according to previous reports [29]. These results underline the need of both silver and nitrate ions for the oxidative cleavage to occur. To further confirm these results, both $AgClO_4$ and $LiNO_3$ (10 mM) were added to the photocatalytic suspension, providing results similar to the run performed in the presence of $AgNO_3$ (Fig. 1).

The essential role of silver ion could be justified by considering its photoinduced reduction to metallic silver onto the semiconductor surface, as demonstrated through HR-TEM and EDX analyses of the photocatalyst recovered after a 180 min lasting run (Fig. 2a-c), and according to what widely reported in literature [30]. Silver nanoparticles of few nanometers, along with some bigger aggregates are visible at the surface of TiO_2. The diffuse reflectance UV–vis spectrum of the same sample (Fig. 2d), besides the band to band transition in the UV region due to TiO_2, shows the typical localized surface plasmon resonance (LSPR) induced absorption band of silver nanoparticles with a maximum centered at ca. 480 nm. Accordingly, the suspension became brownish upon UV-A irradiation.

The electron-induced reduction of silver ion into metal silver nanoparticles could play an important role in addressing the selectivity of the reaction, as it efficiently competes with the reduction of molecular oxygen, which is thermodynamically less favoured. On the other hand, once generated, silver nanoparticles could act as electron-sinks, inhibiting the recombination of the photogenerated electron-hole pairs, and promoting the availability of holes for the oxidation processes [30]. Further investigation is ongoing to clarify these aspects.

Nitrate radicals can be produced upon hole-induced oxidation of nitrate ions according to Eq. (3) [23,24].

$$NO_3^- + h^+ \rightarrow NO_3^{\cdot} \quad (3)$$

The reaction of nitrate radical with unsaturated compounds is briefly summarized in Eqs. (4)–(7), in analogy with the mechanistic hypotheses proposed in previous reports on atmospheric chemistry [31]. Nitrate radical selectively adds to the carbon-carbon double bond, forming an alkyl radical (Eq. (4)), which in turn reacts with molecular oxygen, giving rise to a peroxyl radical (Eq. (5)).

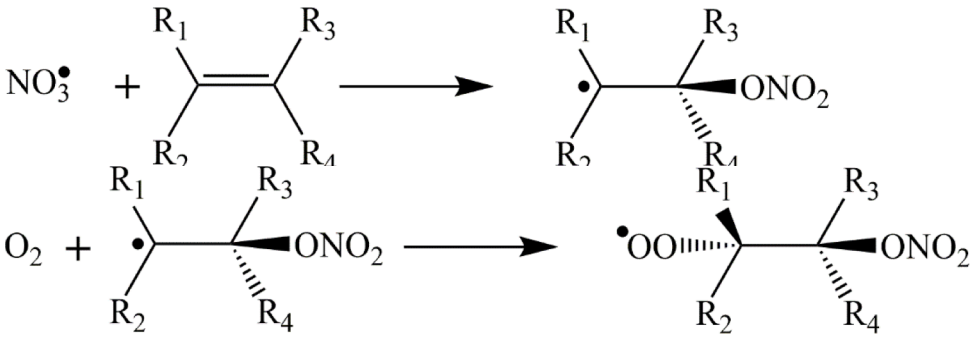

(4)

(5)

This unstable radical, leads to the formation of an alkoxy radical due to the reaction with another nitrate (or peroxyl) radical, producing at the same time molecular oxygen and NO_2 (Eq. (6)). Finally, the alkoxy radical rearranges with the homolytic rupture of the carbon-carbon bond resulting in carbonyl compounds and a NO_2 molecule (Eq. (7)).

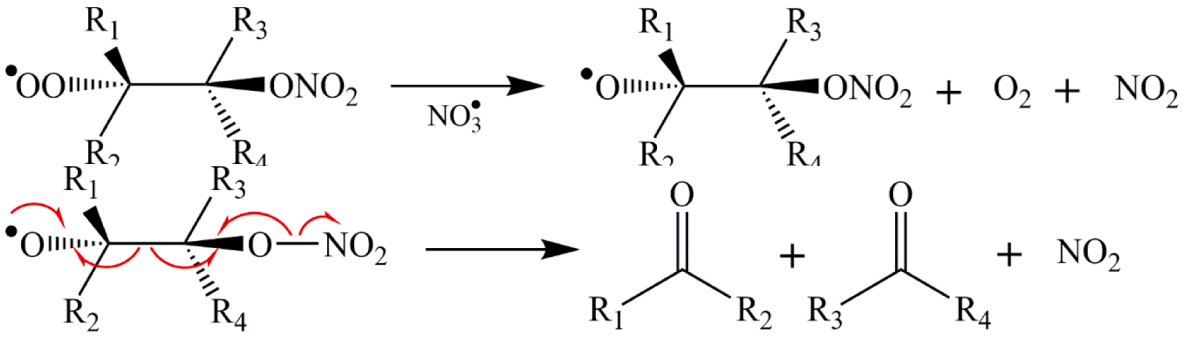

(6)

(7)

To confirm the above proposed mechanism (Eq. (4)-(7)), the formation of nitrogen dioxide (NO_2) has been verified by means of the Griess test. To this aim, the reaction was carried out under flowing air and the gaseous stream exiting the reactor was bubbled throughout a Griess solution. The absorbance of the pink-red dye, formed by the azo-coupling reaction, was measured by means of UV–vis spectroscopy ($\lambda_{max} = 549$ nm) and correlated to the amount of NO_2 produced during the photocatalytic process (see Section S4). Results of a representative run, along with blank tests under flowing nitrogen and in the absence of limonene, are reported in Fig. 3.

In the absence of limonene under air flow, negligible amounts of NO_2 could be detected. Instead, NO_2 was produced in the presence of limonene both under flowing air and N_2, but with different trends. In fact, after a short transitory, NO_2 production was linear ($R^2 = 0.997$) for the entire duration of the experiment under flowing N_2. On the other hand, in the presence of air, the trend was exponential when limonene was present in the photocatalytic suspension (up to ca. 200 min), while it became linear after complete conversion of limonene. The differences in the trends could be tentatively attributed to the fact that only in the presence of oxygen the reaction can proceed through Eq. (5), paving the oxidative cleavage of limonene and the consequent NO_2 production according to Eqs. (6)-(7). On the other hand, NO_2 production can be attributed to nitrate reduction in the absence of oxygen [32]. Accordingly, the trend of NO_2 production was linear both under nitrogen in the presence of limonene and under air in the absence of limonene, indicating similar reaction kinetics. Notably, as above mentioned, limonene did not appreciably react under N_2 atmosphere, even if NO_2 was evolving during the run. This finding allows excluding, under the present conditions, a concurrent NO_2 mediated oxidation of limonene, elsewhere proposed [33]. In order to further corroborate the proposed mechanism, additional experiments were conducted using t-BuOH and HCOOH as OH radicals and holes scavengers, respectively. Results are presented in Fig. S5 of the Supporting Information. Interestingly, the

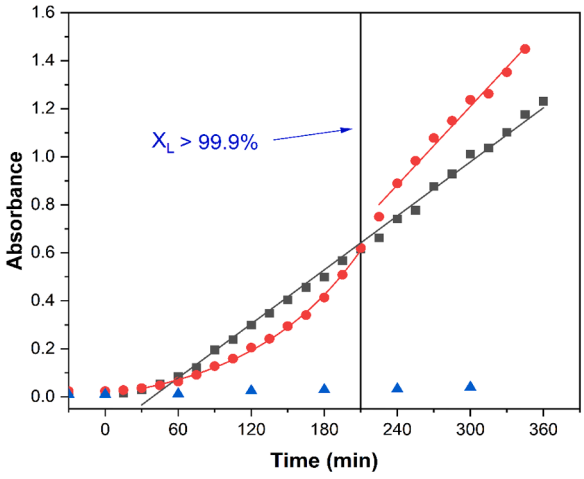

Fig. 3. Absorbance of the Griess solution, indicating nitrogen dioxide formation over time for representative photocatalytic runs under flowing air (red circles), flowing nitrogen (black squares), and for a blank test performed in the absence of limonene under flowing air (blue triangles).

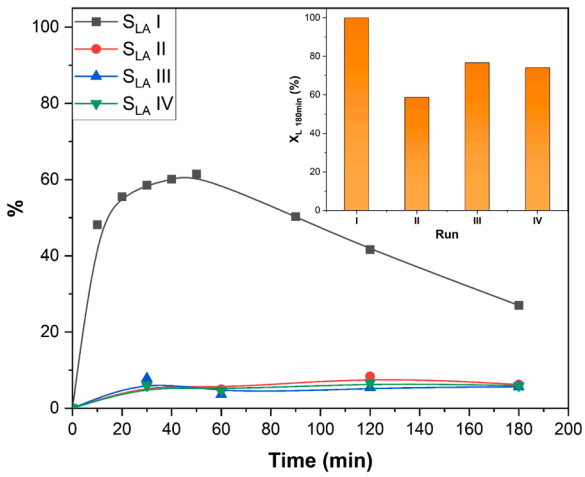

Fig. 4. Selectivity towards limononaldehyde (LA) during irradiation time obtained in four consecutive runs, indicated with roman numerals. The inset shows the corresponding limonene conversion values (X_L) obtained after 180 min of irradiation for each consecutive run.

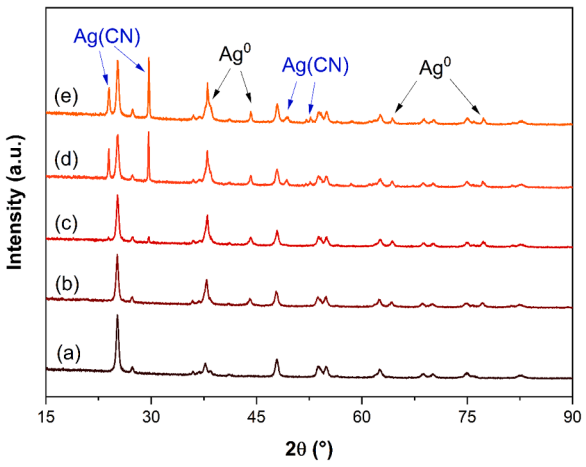

Fig. 5. PXRD patterns of the fresh photocatalyst (a), and of the photocatalyst recovered after 60 (b), 120 (c), 180 (d) minutes of irradiation in a representative run. Pattern (e) is relative to the photocatalyst recovered after the first reuse run, which lasted 180 min.

selectivity and conversion remain virtually unaltered in the presence of t-BuOH, indicating that limononaldehyde does not originate from reactions involving OH radicals and that formation of nitrate radicals is not mediated by OH radicals, as hypothesized in a previous paper [24]. Conversely, in the presence of HCOOH, both the conversion and selectivity values experience a notable reduction. This can be attributed to the competition between nitrate and formate ions for the photogenerated holes, which hampers the oxidation of nitrate anions to nitrate radicals, as well as the direct oxidation of limonene at the catalyst surface. These evidences further confirm that (i) nitrate radicals are formed through hole-induced oxidation of nitrate ions, and that (ii) the oxidative cleavage of olefins is driven by nitrate radicals.

The possibility of reusing the photocatalyst in consecutive runs has been investigated following the procedure detailed in the experimental part. Results are shown in Fig. 4.

The conversion of limonene after 180 min of irradiation (see inset) decreased to ca. 60% during the second run, but it stabilized to ca. 70% during the following repetitions. However, the maximum selectivity to limononaldehyde dramatically fell down from the 60% obtained during the first run to about the 10% of the following runs. At the same time the color of the photocatalyst progressively lightens by performing multiple repetition runs. It is worth to remember that the runs after the first were carried out without further addition of silver ions by adding lithium nitrate as the nitrate radical precursor. Moreover, runs performed in the absence of silver ions but in the presence of TiO_2 previously decorated with silver nanoparticles, show similar low values of selectivity towards limononaldehyde. These evidences strongly corroborate, as above specified, the crucial role of the initial silver ion reduction step in the formation of limononaldehyde. Specifically, silver ions serve as sacrificial electron acceptors, impeding the reduction of molecular oxygen and thereby allowing it to participate in limononaldehyde formation as described in Eq. (5). Moreover, the preferential reduction of silver ions compared to molecular oxygen can enhance the generation of nitrate radicals due to the resulting improved spatial charge separation.

To gain deeper insights into the reason of the selectivity reduction in consecutive runs, we acquired the powder X-ray diffraction patterns of the photocatalyst recovered at various irradiation times during the first run (Fig. 5, patterns a-d) and after the first reuse run, which lasted 180 min (Fig. 5 pattern e).

Along with the characteristic patterns of the crystalline phases of P25 (i.e., anatase and rutile), formation of metallic silver is evident after 60 min of irradiation. Accordingly, the color of the suspension turns from white to brownish, already after the first minutes of irradiation. Moreover, after 120 min of irradiation (pattern c in Fig. 5) it becomes apparent the formation of novel diffraction patterns, which increase in intensity during irradiation (pattern d) and after the first repetition run (pattern e in Fig. 5). These signals have been attributed to solid Ag(CN), which deposited onto the catalyst, being not soluble in acetonitrile. Formation of Ag(CN) can be rationalized by considering the photocatalytic oxidation of acetonitrile, which generally occurs at low extent in irradiated TiO_2 suspensions, thus justifying the common use of acetonitrile in many photocatalytic organic syntheses [34–36]. Accordingly, Friedman et al. [16] claim that acetonitrile cannot be oxidised by the photogenerated holes of common semiconductors. On the contrary, Davit et al. [37] reported relatively small values (up to $1.4 \bullet 10^{-9}$ M/s m^2) of initial rate of acetonitrile photocatalytic degradation in water, per square meter of TiO_2 P25. Litchin and Avudaithai [38] found cyanogen $(CN)_2$ as an intermediate product of the photocatalytic degradation of acetonitrile, and proposed the formation of CN• radicals as reaction intermediates, which readily dimerize. Augugliaro et al. [39] found only traces of cyanide CN^- in the aqueous phase as an acetonitrile oxidation product, possibly because of the stripping of HCN species in gas phase. However, the detected isocyanate and/or cyanate species, were a clear clue of the existence of free cyanide ions. It is worth to mention that, in the present system, the electrophilic attack of nitrate radicals to the triple bond of acetonitrile cannot be excluded, even if less favoured with respect to that to the double bond of limonene. On the basis of this brief literature review, the formation of Ag(CN) in the present system can be rationalized both from reaction of Ag^+ present in solution and the formed CN^-, or by reaction of metallic silver photodeposited onto the photocatalyst with CN• radicals. However, the latter hypothesis seems more likely, as below discussed. In order to shine light on the mechanism underlying this parasitic reaction and its influence on the photocatalytic reaction, Rietveld analysis of the XRD patterns has been performed as shown in Fig. S6 of the Supporting information. The obtained quantitative values of the amount (in weight%, with respect to the mass of photocatalyst) of both metallic silver and Ag(CN) solid phases have been plotted against irradiation time for the first run in Fig. 6, along with the concentration of limonene measured in the liquid phase (right axis).

While, as expected, formation of metallic silver begins immediately upon switching on the lamps, the amount of Ag(CN) is initially negligible and significantly increases up to 15 wt% only after the complete consumption of limonene. This finding demonstrates that the influence of the parasitic formation of Ag(CN) on the photocatalytic activity in the first run is virtually negligible. In fact, limonene can be hypothesized to

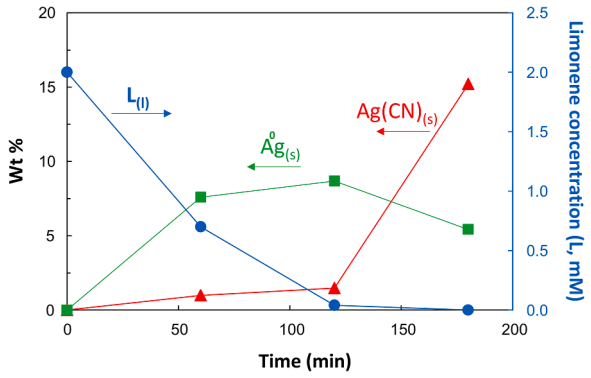

Fig. 6. Amount (wt%) of metallic silver (green squares) and Ag(CN) (red triangles) deposited onto the photocatalyst at selected irradiation times during a representative run, along with the limonene concentration measured in the liquid phase (blue circles, right axis).

efficiently compete (directly through hole-oxidation or indirectly through nitrate radicals) with the oxidation of acetonitrile, which is significantly suppressed in its presence. Moreover, the reduction of the amount of metallic silver occurs after 120 min, concomitantly with the steep increase of the amount of Ag(CN), thus supporting the hypothesis that Ag(CN) is likely formed by reaction of metallic silver and cyanide radicals. This information further explains the lightning of the photocatalyst and the loss in selectivity observed upon multiple reuse. Accordingly the amount of Ag(CN) increases from 15 wt% at the end of the first run to 17.5 wt% at the end of the first reuse, while the amount of metallic silver decreases from 5.4 to 3.8 wt% (see Fig. S6).

The parasitic formation of Ag(CN) poses additional challenges for process optimization in industrial scale-up scenarios. This issue can be readily addressed by utilizing "greener" and more stable solvents, other noble metals (e.g., Pt, Pd) pre-deposited on the P25 surface, combined in-continuous systems and/or photoelectrocatalytic approaches. All of these aspects are the object of future investigations.

It is worth mentioning, that only the endocyclic bond of limonene undergoes cleavage, while the exocyclic bond is stable under the present reaction conditions, in agreement with previously reported theoretical calculations regarding the addition of nitrate radical on the two double bonds [40]. Even though this confers regioselectivity to the present reaction, it indicates the relevance of the nature of the double bond of the olefinic substrate. To clarify this aspect, some other alkene molecules have been tested under the same experimental conditions described above. The tested alkenes are listed in Table 1, along with the obtained product of cleavage, the highest values of selectivity and the corresponding conversion obtained at the indicated irradiation times.

Entries 1–2 present endocyclic double bonds of different nature. Out of them, only limonene (Entry 1) presents a tertiary carbon involved in the double bond. The stability of the resulting intermediate radical (Eq. (4)) justifies the fast conversion (almost complete after 120 min, see Fig. 1) and the highest value of selectivity obtained only after 50 min of irradiation. Instead, the secondary carbons involved in the double bond of cyclohexene (Entry 2) display similar activity in terms of conversion, but lower selectivity (achieved at longer irradiation times) compared with limonene. The cleavage reaction does not take place at all for the electron poor double bond of 2-cyclohexen-1-one, whose degradation is negligible during 180 min irradiation. Entry 3 is a linear alkene with internal double bond, which displays an activity similar to cyclohexene. Notably, the terminal bond of 1-octene does not undergo cleavage. On the other hand, the presence of the aromatic ring activates the terminal bond of styrene (Entry 4), and, accordingly, the activity and selectivity values of stilbene (Entry 5) are higher compared with those of styrene.

Notably, due to the high reactivity of the carbonyl functionality, the cleavage products may undergo polymerization through condensation and cyclization reactions, when present above a certain concentration in the reaction medium. Even though this limits the obtainable yields in batch systems, it suggests that performing them in continuous systems, and by coupling them with membrane separation units, could dramatically benefit the reaction performances [41]. This approach has been successfully implemented for other photocatalytic partial oxidation reactions. Moreover, the produced NO_2 could be easily reoxidized to nitrate anions and reused for subsequent reactions, thus endowing the reaction with high mass efficiency, in accomplishment with the principles of green chemistry [42]. Unfortunately, the sacrificial use of silver ions could limit the practical application of the reaction in the present experimental conditions, but investigation is ongoing to provide suitable alternatives. On the other hand, this finding clearly indicates that the reaction selectivity can be addressed once provided a way to efficiently (and cheaply) compete with molecular oxygen for the photogenerated electrons. Furthermore, it suggests that the formation of nitrate radicals in photocatalytic systems becomes relevant when the oxidizing ability of

Table 1
Highest selectivity (S) and conversion values (X) obtained at the indicated irradiation times (t) for the C=C cleavage reactions of different alkenes.

Entry	Reactant	Cleavage product	X (%)	S (%)	t (min)
1	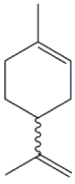	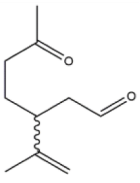	60	60	50
2		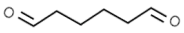	82	37	180
3	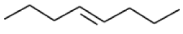	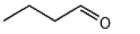	81	38	180
4	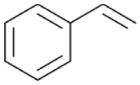	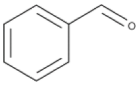	80	25	180
5	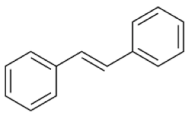	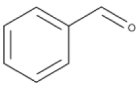	95	37	90

the photogenerated hole is boosted in terms of increased life-time as in the present case, by adding an efficient electron acceptor, or by increasing its redox potential. This is the case of the synthesis of elemental bromine, which is reported to occur efficiently only at acidic value of pH in water [43].

4. Conclusions

The C=C cleavage reaction of alkenes induced by nitrate radicals photocatalytically generated can be considered a viable alternative to the existing analogous processes. The reaction is general, with the exception of compounds bearing electron poor and terminal double bonds. Under the described experimental conditions, the initial reduction of silver as a sacrificial electron scavenger is essential for the formation of the carbonyl compounds. Moreover, the parasitic formation of Ag(CN) on the catalyst surface, even if significant only after the complete consumption of the olefin, requires further optimization and refinement of the system. Nonetheless, results constitute indirect evidence of the possibility of generating and using nitrate radicals in heterogeneous photocatalytic systems, and can be considered as the starting point for novel nitrate radical based photocatalytic syntheses towards a sustainable production of industrially relevant compounds.

CRediT authorship contribution statement

Alessandro Gottuso: Investigation, Validation, Methodology, Writing – review & editing. **Claudio De Pasquale:** Validation, Resources. **Stefano Livraghi:** Methodology, Writing – review & editing. **Leonardo Palmisano:** Supervision, Writing – review & editing. **Sandra Diré:** Data curation, Formal analysis, Methodology. **Riccardo Ceccato:** Data curation, Formal analysis. **Francesco Parrino:** Conceptualization, Methodology, Writing – original draft, Writing – review & editing, Supervision.

Declaration of Competing Interest

The authors declare the following financial interests/personal relationships which may be considered as potential competing interests: Francesco Parrino has patent #102022000025980 pending to Assignee. Also Alessandro Gottuso, Claudio De Pasquale, Leonardo Palmisano, Riccardo Ceccato and Sandra Dirè are co-inventors of the Patent 102022000025980.

Data availability

Data will be made available on request.

Acknowledgement

This contribution is dedicated to Prof. Rosario Pietropaolo, a visionary of science, master of ethics and dedication and inspiration for many of us.

Supplementary materials

Supplementary material associated with this article can be found, in the online version, at doi:10.1016/j.mcat.2023.113607.

References

[1] a) J.-E. Bäckvall, Modern Oxidation Methods, Wiley-VCH, Weinheim, 2010;
b) P.G. Andersson, I.J. Munslow, Modern Reduction Methods, Wiley-VCH, Weinheim, 2008;
c) I. Amghizar, L.A. Vandewalle, K.M. Van Geem, G.B. Marin, New trends in olefin production, Engineering 3 (2017) 171, https://doi.org/10.1016/J.ENG.2017.02.006.

[2] Z. Huang, R. Guan, M. Shanmugam, E.L. Bennett, C.M. Robertson, A. Brookfield, E. J.L. McInnes, J. Xiao, Oxidative cleavage of alkenes by O_2 with a non-heme manganese catalyst, J. Am. Chem. Soc. 143 (2021) 10005, https://doi.org/10.1021/jacs.1c05757.

[3] A. Rajagopalan, M. Lara, W. Kroutil, Oxidative alkene cleavage by chemical and enzymatic methods, Adv. Synth. Catal. 355 (2013) 3321, https://doi.org/10.1002/adsc.201300882.

[4] a) K. Takada, K. Fuchise, N. Kubota, T. Ito, Y. Chen, T. Satoh, T. Kakuchi, Synthesis of α-, ω-, and α,ω-end-functionalized poly(n-butyl acrylate)s by organocatalytic group transfer polymerization using functional initiator and terminator, Macromolecules 47 (2014) 5514, https://doi.org/10.1021/ma501106e;
b) M.-J. Tenorio, R.V. Chaudhari, B. Subramaniam, Rh-catalyzed hydroformylation of 1,3-butadiene and pent-4-enal to adipaldehyde in CO_2-expanded media, Ind. Eng. Chem. Res. 58 (2019) 22526, https://doi.org/10.1021/acs.iecr.9b05184;
c) J. Mormul, M. Mulzer, T. Rosendahl, F. Rominger, M. Limbach, P. Hofmann, Synthesis of adipic aldehyde by n-selective hydroformylation of 4-pentenal, Organometallics 34 (2015) 4102, https://doi.org/10.1021/acs.organomet.5b00538;
d) Q. Li, Z. Zhang, J. Zhao, A. Li, Recent advances in the sustainable production of α,ω-C_6 bifunctional compounds enabled by chemo-/biocatalysts, Green Chem. 24 (2022) 4270, https://doi.org/10.1039/D2GC00288D.

[5] K.N. Parida, J.N. Moorthy, Oxidation cascade with oxone: cleavage of olefins to carboxylic acids, Tetrahedron 70 (2014) 2280, https://doi.org/10.1016/j.tet.2014.01.042.

[6] P. Viski, Z. Szeverenyi, L.I. Simandi, A novel procedure for the cleavage of olefin derivatives to aldehydes using potassium permanganate, J. Org. Chem. 51 (1986) 3213, https://doi.org/10.1021/jo00366a029.

[7] F. Mecozzi, J.J. Dong, D. Angelone, W.R. Browne, N.N.H.M. Eisink, Oxidative cleavage of alkene C=C bonds using a manganese catalyzed oxidation with H_2O_2 combined with periodate oxidation, Eur. J. Org. Chem. (2019) 7151, https://doi.org/10.1002/ejoc.201901380.

[8] S. Jarupinthusophon, U. Thong-In, W. Chavasiri, Catalytic oxidative cleavage of terminal olefins by chromium (III) stearate, J. Mol. Catal. A: Chem. 270 (2007) 289, https://doi.org/10.1016/j.molcata.2007.02.007.

[9] D.S. Nesterov, O.V. Nesterova, Catalytic oxidations with meta-chloroperoxybenzoic acid (m-CPBA) and mono- and polynuclear complexes of nickel: a mechanistic outlook, Catalysts 11 (2021) 148, https://doi.org/10.3390/catal11101148.

[10] U. Atmaca, H.K. Usanmaz, M. Çelik, Oxidations of alkenes with hypervalent iodine reagents: an alternative ozonolysis of phenyl substituted alkenes and allylic oxidation of unsubstituted cyclic alkenes, Tetrahedron Lett. 55 (2014) 2230, https://doi.org/10.1016/j.tetlet.2014.02.076.

[11] a) H. Werner, E. Bleuel, Metal-assisted cleavage of a C−C double bond: Simple and reversible, Angew. Chem. Int. Ed. 40 (2001) 145, https://doi.org/10.1002/1521-3773(20010105)40:1;
b) G.A.-O. Frost, M.N. Mittelstaedt, C.A.-O. Douglas, Chemoselectivity for alkene cleavage by palladium-catalyzed intramolecular diazo group transfer from azide to alkene, Org. Lett. 8 (2006) 693, https://doi.org/10.1002/chem.201805904;
c) B.R. Travis, R.S. Narayan, B. Borhan, Osmium tetroxide-promoted catalytic oxidative cleavage of olefins: an organometallic ozonolysis, J. Am. Chem. Soc. 124 (2002) 824, https://doi.org/10.1021/ja017295g.

[12] S.-T. Liu, K.V. Reddy, R.-Y. Lai, Oxidative cleavage of alkenes catalyzed by a water/organic soluble manganese porphyrin complex, Tetrahedron 63 (2007) 1821, https://doi.org/10.1016/j.tet.2006.12.029.

[13] a) T.J. Fisher, P.H. Dussault, Alkene ozonolysis, Tetrahedron 73 (2017) 4233, https://doi.org/10.1016/j.tet.2017.03.039S;
b) G. Van Ornum, R.M. Champeau, R. Pariza, Ozonolysis applications in drug synthesis, Chem. Rev. 106 (2006) 2990, https://doi.org/10.1021/cr040682z;
c) N.M. Donahue, J.E. Tischuk, B.J. Marquis, K.E. Huff Hartz, Secondary organic aerosol from limona ketone: insights into terpene ozonolysis via synthesis of key intermediates, Phys. Chem. Chem. Phys. 9 (2007) 2991, https://doi.org/10.1039/B701333G;
d) M.L. Walser, Y. Desyaterik, J. Laskin, A. Laskin, S.A. Nizkorodov, High-resolution mass spectrometric analysis of secondary organic aerosol produced by ozonation of limonene, Phys. Chem. Chem. Phys. 10 (2008) 1009, https://doi.org/10.1039/B712620D;
e) S. Leungsakul, M. Jaoui, R.M. Kamens, Kinetic mechanism for predicting secondary organic aerosol formation from the reaction of D-limonene with ozone, Environ. Sci. Technol. 39 (2005) 9583, https://doi.org/10.1021/es0492687.

[14] a) R.S. Murthy, M. Bio, Y. You, Low energy light-triggered oxidative cleavage of olefins, Tetrahedron Lett 50 (2009) 1041, https://doi.org/10.1016/j.tetlet.2008.12.069;
b) E.L. Clennan, A. Pace, Advances in singlet oxygen chemistry, Tetrahedron 61 (2005) 6665, https://doi.org/10.1016/j.tet.2005.04.017.

[15] R. Franke, D. Selent, A. Börner, Applied hydroformylation, Chem. Rev. 112 (2012) 5675, https://doi.org/10.1021/cr3001803.

[16] a) D. Friedmann, A. Hakki, H. Kim, W. Choi, D. Bahnemann, Heterogeneous photocatalytic organic synthesis: state-of-the-art and future perspectives, Green Chem. 18 (2016) 5391, https://doi.org/10.1039/C6GC01582D;
b) F. Parrino, L. Palmisano, Reactions in the presence of irradiated semiconductors: are they simply photocatalytic? Mini-Rev. Org. Chem. 15 (2018) 157, https://doi.org/10.2174/1570193X14666171117151718.

[17] H. Kisch, Semiconductor photocatalysis: Principles and applications 2015, 1–249.

[18] X. Wang, Y. Li, Z. Li, Thiol-initiated photocatalytic oxidative cleavage of the C=C bond in olefins and its extension to direct production of acetals from olefins, Catal. Sci. Technol. 11 (2021) 1000, https://doi.org/10.1039/D0CY01963A.
[19] Y. Deng, X.-J. Wei, H. Wang, Y. Sun, T. Noël, X. Wang, Disulfide-catalyzed visible light-mediated oxidative cleavage of C=C bonds and evidence of an olefin–disulfide charge-transfer complex, Angew. Chem. Int. Ed. 56 (2017) 832, https://doi.org/10.1002/anie.201607948.
[20] Y. Zhang, N. Hatami, N.S. Lange, E. Ronge, W. Schilling, C. Jooss, S. Das, A metal-free heterogeneous photocatalyst for the selective oxidative cleavage of C=C bonds in aryl olefins via harvesting direct solar energy, Green Chem. 22 (2020) 4516–4522, https://doi.org/10.1039/D0GC01187H.
[21] T. Liu, F. Xue, Z. Chen, Z. Cheng, W. Cao, B. Wang, W. Jin, Y. Xia, Y. Zhang, C. Liu, $Bi_4O_5Br_2$ catalyzed selective oxidative of C=C double bonds to ketones with molecular oxygen under visible-light irradiation, J. Catal. 414 (2022) 76–83, https://doi.org/10.1016/j.jcat.2022.08.029.
[22] F. Parrino, S. Dirè, R. Ceccato, A. Gottuso, L. Palmisano, C. De Pasquale, patent n°102022000025980 filed on 19-12-2022.
[23] F. Parrino, S. Livraghi, E. Giamello, L. Palmisano, The existence of nitrate radicals in irradiated TiO_2 aqueous suspensions in the presence of nitrate ions, Angew. Chem. Int. Ed. 57 (2018) 10702, https://doi.org/10.1002/anie.201804879.
[24] F. Parrino, S. Livraghi, E. Giamello, R. Ceccato, L. Palmisano, Role of hydroxyl, superoxide, and nitrate radicals on the fate of bromide ions in photocatalytic TiO_2 suspensions, ACS Catal 10 (2020) 7922, https://doi.org/10.1021/acscatal.0c02010.
[25] J.L. Di Meglio, A.G. Breuhaus-Alvarez, S. Li, B.M. Bartlett, Nitrate-mediated alcohol oxidation on cadmium sulfide photocatalysts, ACS Catal., 9 (2019) 5732, https://doi.org/10.1021/acscatal.9b01051.
[26] B. Othani, O.O. Prieto-Mahaney, D. Li, R. Abe, What is Degussa (Evonik) P25? Crystalline composition analysis, reconstruction from isolated pure particles and photocatalytic activity test, J. Photochem. Photobiol. A 216 (2010) 179–182, https://doi.org/10.1016/j.jphotochem.2010.07.024.
[27] L. Lutterotti, "MAUD (Material Analysis Using Diffraction) version 2.33," 2010. http://maud.radiographema.eu.
[28] a) A. Abd-Elaal, F. Parrino, R. Ciriminna, V. Loddo, L. Palmisano, M. Pagliaro, Alcohol selective oxidation in water under mild conditions via a novel approach to hybrid composite photocatalysts, Chem. Open 4 (2015) 779–785, https://doi.org/10.1002/open.201500110;
b) H. Khlifi, F. Parisi, L. Elsellami, G. Camera-Roda, L. Palmisano, R. Ceccato, F. Parrino, Photocatalytic partial oxidation of tyrosol: improving the selectivity towards hydroxytyrosol by surface fluorination of TiO_2, Top. Catal. 63 (2020) 1350, https://doi.org/10.1007/s11244-020-01287-y.
[29] a) R. Ciriminna, F. Parrino, C. De Pasquale, L. Palmisano, M. Pagliaro, Photocatalytic partial oxidation of limonene to 1,2 limonene oxide, Chem. Commun. 54 (2018) 1008, https://doi.org/10.1039/C7CC09788C;
b) A. Gottuso, A. Köckritz, M.L. Saladino, F. Armetta, C. De Pasquale, G. Nasillo, F. Parrino, Catalytic and photocatalytic epoxidation of limonene: using mesoporous silica nanoparticles as functional support for a Janus-like approach, J. Catal. 391 (2020) 202, https://doi.org/10.1016/j.jcat.2020.08.025.
[30] Z. Wei, M. Janczarek, M. Endo, C. Colbeau-Justin, B. Ohtani, E. Kowalska, Silver-modified octahedral anatase particles as plasmonic photocatalyst, Catal. Today 310 (2018) 19, https://doi.org/10.1016/j.cattod.2017.05.039.
[31] a) R.P. Wayne, I. Barnes, P. Biggs, J.P. Burrows, C.E. Canosa-Mas, J. Hjorth, G. Le Bras, G.K. Moortgat, D. Perner, G. Poulet, G. Restelli, H. Sidebottom, The nitrate radical: physics, chemistry, and the atmosphere, Atm. Environ. A. Gen. Top. 25 (1991) 1, https://doi.org/10.1016/0960-1686(91)90192;
b) A.S.P. Mezyk, T.D. Cullen, K.A. Rickman, B.J. Mincher, The reactivity of the nitrate radical (NO_3) in aqueous and organic solutions, Int. J. Chem. Kin. 49 (2017) 635, https://doi.org/10.1002/kin.21103;
c) L.M. Smith, H.M. Aitken, M.L. Coote, The fate of the peroxyl radical in autoxidation: how does polymer degradation really occur? Acc. Chem. Res. 51 (2018) 2006, https://doi.org/10.1021/acs.accounts.8b00250;
d) J.J. Orlando, G.S. Tyndall, Laboratory studies of organic peroxy radical chemistry: an overview with emphasis on recent issues of atmospheric significance, Chem. Soc. Rev. 41 (2012) 6294, https://doi.org/10.1039/C2CS35166H;
e) F. Kirchner, W.R. Stockwell, Effect of peroxy radical reactions on the predicted concentrations of ozone, nitrogenous compounds, and radicals, J. Geophys. Res: Atm. 101 (1996) 21007, https://doi.org/10.1029/96JD01519.
[32] T.L. Broder, D.S. Silvester, L. Aldous, C. Hardacre, A. Crossley, R.G. Compton, The electrochemical oxidation and reduction of nitrate ions in the room temperature ionic liquid [C_2mim][NTf_2]; the latter behaves as a 'melt' rather than an 'organic solvent, New J. Chem. 31 (2007) 966, https://doi.org/10.1039/B701097D.
[33] a) W.A. Pryor, J.W. Lightsey, D.F. Church, Reaction of nitrogen dioxide with alkenes and polyunsaturated fatty acids: addition and hydrogen-abstraction mechanisms, J. Am. Chem. Soc. 104 (1982) 6685, https://doi.org/10.1021/ja00388a035;
b) A. Rubinstein, P. Jiménez-Lozanao, J.J. Carbó, J.M. Poblet, R. Neumann, Aerobic carbon–carbon bond cleavage of alkenes to aldehydes catalyzed by first-row transition-metal-substituted polyoxometalates in the presence of nitrogen dioxide, J. Am. Chem. Soc. 136 (2014) 10941, https://doi.org/10.1021/ja502846h.
[34] J. Colmenares, W. Ouyang, M. Ojeda, E. Kuna, O. Chernyayeva, D. Lisovytskiy, S. De, R. Luque, A. Balu, Mild ultrasound-assisted synthesis of TiO_2 supported on magnetic nanocomposites for selective photo-oxidation of benzyl alcohol, Appl. Catal. B: Environ. 183 (2016) 107, https://doi.org/10.1016/j.apcatb.2015.10.034.
[35] W. Mu, J.M. Herrmann, P. Pichat, Room temperature photocatalytic oxidation of liquid cyclohexane into cyclohexanone over neat and modified TiO_2, Catal. Lett. 3 (1989) 73, https://doi.org/10.1007/BF00765057.
[36] M. Huang, H. Guo, Z. Zeng, H. Xiao, H. Hu, L. He, K. Li, X. Liu, L. Yan, Selective photocatalytic transformation of lignin to aromatic chemicals by crystalline carbon nitride in water–acetonitrile solutions, Int. J. Environ. Res. Public Health 19 (2022) 15707, https://doi.org/10.3390/ijerph192315707.
[37] P. Davit, G. Martra, S. Coluccia, V. Augugliaro, E. García, López, V. Loddo, G. Marcì, L. Palmisano, M. Schiavello, Adsorption and photocatalytic degradation of acetonitrile: FT-IR investigation, J. Mol. Catal. A: Chem. 204–205 (2003) 693, https://doi.org/10.1016/S1381-1169(03)00354-6.
[38] N.N. Litchin, M. Avudaithai, TiO_2-photocatalyzed oxidative degradation of CH_3CN, CH_3OH, C_2HCl_3, and CH_2Cl_2 supplied as vapors and in aqueous solution under similar conditions, Environ. Sci. Technol. 6 (1996) 2014, https://doi.org/10.1021/es950816d.
[39] V. Augugliaro, A. Bianco Prevot, J. Cáceres Vázquez, E. García-López, A. Irico, V. Loddo, S. Malato Rodríguez, G. Marcì, L. Palmisano, E. Pramauro, Photocatalytic oxidation of acetonitrile in aqueous suspension of titanium dioxide irradiated by sunlight, Adv. Environ. Res. 8 (2004) 329, https://doi.org/10.1016/S1093-0191(02)00106-5.
[40] L. Jiang, W. Wang, Y.S. Xu, Theoretical investigation of the NO_3 radical addition to double bonds of limonene, Int. J. Mol. Sci. 10 (2009) 3743, https://doi.org/10.3390/ijms10093743.
[41] a) G. Camera-Roda, V. Loddo, L. Palmisano, F. Parrino, F. Santarelli, Process intensification in a photocatalytic membrane reactor: Analysis of the techniques to integrate reaction and separation, Chem. Eng. J. 310 (2017) 352, https://doi.org/10.1016/j.cej.2016.06.019G;
b) A. Cardillo, G. Camera-Roda, V. Loddo, L. Palmisano, F. Parrino, Improvement of membrane performances to enhance the yield of vanillin in a pervaporation reactor, Membranes 4 (2014) 96, https://doi.org/10.3390/membranes4010096;
c) M. Bellardita, G. Camera-Roda, V. Loddo, F. Parrino, L. Palmisano, Coupling of membrane and photocatalytic technologies for selective formation of high added value chemicals, Catal. Today 340 (2020) 128, https://doi.org/10.1016/j.cattod.2018.09.024.
[42] B.M. Trost, The atom economy—a search for synthetic efficiency, Science 254 (1991) 1471, https://doi.org/10.1126/science.1962206.
[43] F. Parrino, G. Camera-Roda, V. Loddo, L. Palmisano, Elemental bromine production by TiO_2 photocatalysis and/or ozonation, Angew. Chem. Int. Ed. 55 (2016) 10391, https://doi.org/10.1002/anie.201603635.